

Relations Between Environments of Quasars and Galaxy Formation

Motohiro ENOKI ^{1,2}, Masahiro NAGASHIMA ², and Naoteru GOUDA ²

¹*Department of Earth and Space Science, Graduate School of Science,
Osaka University, Toyonaka, Osaka, 560-0043*

²*National Astronomical Observatory, Osawa 2-21-1, Mitaka, Tokyo, 181-8588
enoki@vega.ess.sci.osaka-u.ac.jp, masa@th.nao.ac.jp, naoteru.gouda@nao.ac.jp*

(Received 2002 August 1; accepted 2002 0)

Abstract

We investigate the environments of quasars such as number distribution of galaxies using a semi-analytic model which includes both galaxy and quasar formations based on the hierarchical clustering scenario. We assume that a supermassive black hole is fueled by accretion of cold gas and that it is a source of quasar activities during a major merger of the quasar host galaxy with another galaxy. This major merger causes spheroid formation of the host galaxy. Our model can reproduce not only galaxy luminosity functions in the local Universe but also the observed relation between a supermassive black hole mass and a spheroid luminosity, and the quasar luminosity functions at different redshifts. Using this model, we predict both the mean number of quasars per halo and the probability distribution of the number of galaxies around quasars. In our model, analysis of the mean number of quasars per halo shows that the spatial distribution of galaxies is different from that of quasars. Furthermore, we found from calculation of the probability distribution of galaxy numbers that at $0.2 \lesssim z \lesssim 0.5$, most quasars are likely to reside in galaxy groups. On the other hand, at $1 \lesssim z \lesssim 2$ most quasars seem to reside in more varied environments than at a lower redshift; quasars reside in environments ranging from small groups of galaxies to clusters of galaxies. Comparing these predictions with observations in future will enable us to constrain our quasar formation model.

Key words: galaxies: evolution — galaxies: formation — galaxies: quasars: general

1. Introduction

The environments of quasars provide important clues to the physical processes of their formation and also yield important information about the relations between the distribution of quasars and the large-scale structure of the universe. For more than three decades, we have known that quasars are associated with enhancements in the spatial distributions of galaxies(Bahcall, Schmidt, Gunn 1969). Studies of the environments of quasars in the nearby universe ($z \lesssim 0.4$) have shown that quasars reside in environments ranging from small to moderate groups of galaxies rather than in rich clusters (e.g. Bahcall, Chokshi 1991; Fisher et al. 1996; McLure, Dunlop 2001). In order to interpret the observational results of the environments of quasars at low redshifts and predict the environments of quasars at high redshifts, a physical model of quasar formation based on cosmological context is required.

It has become widely accepted that quasars are fueled by accretion of gas onto supermassive black holes (SMBHs) in the nuclei of host galaxies since Lynden-Bell (1969) proposed this idea on quasars. Recent observations of galactic centers suggest that a lot of nearby galaxies have central black holes and their estimated masses correlate with the luminosities of spheroids¹ of their host galaxies (e.g. Kormendy, Richstone 1995; Magorrian et al. 1998; Merritt, Ferrarese 2001). The connection between SMBHs and their host spheroids suggests that the formation of SMBHs physically links the formation of the spheroids which harbor the SMBHs. Thus, this implies that the formation of quasars is closely related to the formation of galaxies, especially of spheroids. Therefore, in order to study the formation and evolution of quasars, it is necessary to construct a unified model which includes both galaxy formation and quasar formation.

Recently, some authors have tried to construct galaxy formation models on the basis of the theory of hierarchical structure formation in cold dark matter (CDM) universe. These efforts are referred to as semi-analytic models (SAMs) of galaxy formation. In the CDM universe, dark matter halos cluster gravitationally and merge together in a manner that depends on the adopted power spectrum of initial density fluctuations. In each of the merged dark halos, radiative gas cooling, star formation, and supernova feedback occur. The cooled dense gas and stars constitute *galaxies*. These galaxies sometimes merge together in a common dark halo and more massive galaxies form. In SAMs, the merger trees of dark matter halos are constructed using a Monte-Carlo algorithm and simple models are adapted to describe the above gas processes. Stellar population synthesis models are used to calculate the luminosities and colors of model galaxies. It is therefore straightforward to understand how galaxies form and evolve within the context of this model. SAMs successfully have reproduced a variety of observed features of local galaxies such as their luminosity functions, color distribution, and so on (e.g. Kauffmann, White, Guiderdoni 1993; Cole et al. 1994, 2000; Somerville, Primack 1999;

¹ Throughout this paper, we refer to bulge or elliptical galaxy as *spheroid*.

Nagashima et al. 2001, 2002).

In these models, it is assumed that disk stars are formed by cooling of gas in the halo. If two galaxies of comparable mass merge, it is assumed that starbursts occur and form the spheroidal component in the center of the galaxy. *N*-body simulations have shown that a merger hypothesis for the origin of spheroids can explain their detailed internal structure (e.g. Barnes 1988; Hernquist 1992, 1993; Heyl, Hernquist, Spergel 1994). Kauffmann and Charlot (1998) have demonstrated that the merger scenario for the formation of elliptical galaxies is consistent with the color-magnitude relation and its redshift evolution (see also Nagashima, Gouda 2001). On the other hand, hydrodynamical simulations have shown that a merger of galaxies drives gas to fall rapidly to the center of a merged system and to fuel nuclear starburst (Negroponte, White 1983; Mihos, Hernquist 1994, 1996; Barnes, Hernquist 1996). Moreover, observed images of quasar hosts show that many quasars reside in interacting systems or elliptical galaxies (Bahcall et al. 1997). Therefore, it has often been thought that the major merger of galaxies would be a possible mechanism for quasar and spheroid formation.

So far, a lot of studies on quasar evolution based on the hierarchical clustering scenario have been carried out with the assumption that the formation of quasars is linked to the first collapse of dark matter halos with galactic mass and that these models can explain the decline of quasar number density at $z \gtrsim 3$ (e.g. Efstathiou, Rees 1988; Haehnelt, Rees 1993) and properties of luminosity functions of quasars (e.g. Haiman, Loeb 1998; Haehnelt, Natarajan, Rees 1998; Hosokawa et al. 2001). However, if quasars are directly linked to spheroids of host galaxies rather than to dark matter halos, the approximation of a one-to-one relation between quasar hosts and dark matter halos would be very crude, especially at low redshift. Therefore, it is necessary to construct a model related to spheroid formation and SMBH formation directly. Kauffmann and Haehnelt (2000) introduced a unified model of the evolution of galaxies and quasars within the framework of SAM (see also Cattaneo 2001). They assumed that SMBHs are formed and fueled during major galaxy mergers and their model reproduces quantitatively the observed relation between spheroid luminosity and black hole mass in nearby galaxies, the strong evolution of the quasar population with redshift, and the relation between the luminosities of nearby quasars and those of their host galaxies.

In this paper, we investigate properties of quasar environments, using a SAM incorporated simple quasar evolution model. We assume that SMBHs are formed and fueled during major galaxy mergers and the fueling process leads quasar activities. While this assumption is similar to the model of Kauffmann, Haehnelt (2000), our galaxy formation model and the adapted model of fueling process are different from their model. Here we focus on optical properties of quasars and attempt to consider the number of quasars per halo and the number of galaxies around quasars as characterizations of environments of quasars, because a) these quantities provide a direct measure of bias in their distribution with respect to galaxies and b) comparing results of the model with observations will enable us to constrain our quasar

formation model.

The paper is organized as follows: in §2 we briefly review our SAM for galaxy formation; in §3 we introduce the quasar formation model; in §4 we calculate the galaxy number distribution function around quasars; in §5 we provide a summary and discussion.

In this study, we use a low-density, spatially flat cold dark matter (Λ CDM) universe with the present density parameter $\Omega_0 = 0.3$, the cosmological constant $\lambda_0 = 0.7$, the Hubble constant in units of $100 \text{ km s}^{-1} \text{ Mpc}^{-1}$ $h = 0.7$ and the present rms density fluctuation in spheres of $8h^{-1}\text{Mpc}$ radius $\sigma_8 = 1.0$.

2. Model of Galaxy Formation

In this section we briefly describe our SAM for the galaxy formation model, details of which are shown in Nagashima et al. (2001). Our present SAM analysis obtains essentially the same results as the previous SAM analyses, with minor differences in a number of details.

First, we construct Monte Carlo realizations of merging histories of dark matter halos using the method of Somerville, Kolatt (1999), which is based on the extended Press-Schechter formalism (Press, Schechter 1974; Bower 1991; Bond et al. 1991; Lacey, Cole 1993). We adopt the power spectrum for the specific cosmological model from Bardeen et al. (1986). Halos with circular velocity $V_{\text{circ}} < 40 \text{ km s}^{-1}$ are treated as diffuse accretion matter. The evolution of the baryonic component is followed until the output redshift coincides with the redshift interval of $\Delta z = 0.06(1+z)$, corresponding to the dynamical time scale of halos which collapse at the redshift z . Note that Shimizu et al. (2002) recently pointed out that a much shorter timestep is required to correctly reproduce the mass function given by the Press-Schechter formalism. However, a serious problem exists only at small mass scales ($\lesssim 10^{11} M_\odot$). Thus we use the above prescription of timestep.

If a dark matter halo has no progenitor halos, the mass fraction of the gas in the halo is given by Ω_b/Ω_0 , where $\Omega_b = 0.015h^{-2}$ is the baryonic density parameter. When a dark matter halo collapses, the gas in the halo is shock-heated to the virial temperature of the halo. We refer to this heated gas as the *hot gas*. At the same time, the gas in dense regions of the halo cools due to efficient radiative cooling. We call this cooled gas the *cold gas*. Assuming a singular isothermal density distribution of the hot gas and using the metallicity-dependent cooling function by Sutherland & Dopita (1991), we calculate the amount of cold gas which eventually falls onto a central galaxy in the halo. In order to avoid the formation of unphysically large galaxies, the above cooling process is applied only to halos with $V_{\text{circ}} < 400 \text{ km s}^{-1}$.

Stars are formed from the cold gas at a rate of $\dot{M}_* = M_{\text{cold}}/\tau_*$, where M_{cold} is the mass of cold gas and τ_* is the time scale of star formation. We assume that τ_* is independent of z , but dependent on V_{circ} as follows:

$$\tau_* = \tau_*^0 \left(\frac{V_{\text{circ}}}{300 \text{ km s}^{-1}} \right)^{\alpha_*}. \quad (1)$$

The free parameters of τ_*^0 and α_* are fixed by matching the observed mass fraction of cold gas in neutral form in the disks of spiral galaxies. In our SAM, stars with masses larger than $10M_\odot$ explode as Type II supernovae (SNe) and heat up the surrounding cold gas. This SN feedback reheats the cold gas to hot gas at a rate of $\dot{M}_{\text{reheat}} = \beta \dot{M}_*$, where β is the efficiency of reheating. We assume that β depends on V_{circ} as follows:

$$\beta = \left(\frac{V_{\text{circ}}}{V_{\text{hot}}} \right)^{-\alpha_{\text{hot}}}. \quad (2)$$

The free parameters of V_{hot} and α_{hot} are determined by matching the local luminosity function of galaxies. With these \dot{M}_* and \dot{M}_{reheat} thus determined, we obtain the masses of hot gas, cold gas, and disk stars as a function of time during the evolution of galaxies. Given the star formation rate as a function of time, the absolute luminosity and colors of individual galaxies are calculated using a population synthesis code by Kodama, Arimoto (1997).

When several progenitor halos have merged, the newly formed larger halo should contain at least two or more galaxies which had originally resided in the individual progenitor halos. We identify the central galaxy in the new common halo with the central galaxy contained in the most massive of the progenitor halos. Other galaxies are regarded as satellite galaxies. These satellites merge by either dynamical friction or random collision. The time scale of merging by dynamical friction is given by

$$\tau_{\text{fric}} = \frac{260}{\ln \Lambda_c} \left(\frac{R_{\text{H}}}{\text{Mpc}} \right)^2 \times \left(\frac{V_{\text{circ}}}{10^3 \text{km s}^{-1}} \right) \left(\frac{M_{\text{sat}}}{10^{12} M_\odot} \right)^{-1} \text{Gyr}, \quad (3)$$

where R_{H} and V_{circ} are the radius and the circular velocity of the new common halo, respectively, $\ln \Lambda_c$ is the Coulomb logarithm, and M_{sat} is the mass of the satellite galaxy including its dark matter halo (Binney, Tremaine 1987). When the time passed after a galaxy becomes a satellite exceeds τ_{fric} , a satellite galaxy infalls onto the central galaxy. On the other hand, the mean free time scale of random collision is given by

$$\tau_{\text{coll}} = \frac{500}{N^2} \left(\frac{R_{\text{H}}}{\text{Mpc}} \right)^3 \left(\frac{r_{\text{gal}}}{0.12 \text{Mpc}} \right)^{-2} \times \left(\frac{\sigma_{\text{gal}}}{100 \text{km s}^{-1}} \right)^{-4} \left(\frac{\sigma_{\text{halo}}}{300 \text{km s}^{-1}} \right)^3 \text{Gyr}, \quad (4)$$

where N is the number of satellite galaxies, r_{gal} is their radius, and σ_{halo} and σ_{gal} are the 1D velocity dispersions of the common halo and satellite galaxies, respectively (Makino, Hut 1997). With a probability of $\Delta t / \tau_{\text{coll}}$, where Δt is the timestep corresponding to the redshift interval Δz , a satellite galaxy merges with another randomly piked satellite.

Consider the case that two galaxies of masses m_1 and $m_2 (> m_1)$ merge together. If the mass ratio $f = m_1/m_2$ is larger than a certain critical value of f_{bulge} , we assume that a starburst occurs and all the cold gas turns into hot gas, which fills the halo, and the stars

Table 1. Model Parameters

cosmological parameters				astrophysical parameters				
Ω_0	λ_0	h	σ_8	V_{hot} (km s $^{-1}$)	α_{hot}	τ_*^0 (Gyr)	α_*	f_{bulge}
0.3	0.7	0.7	1	280	2.5	1.5	-2	0.5

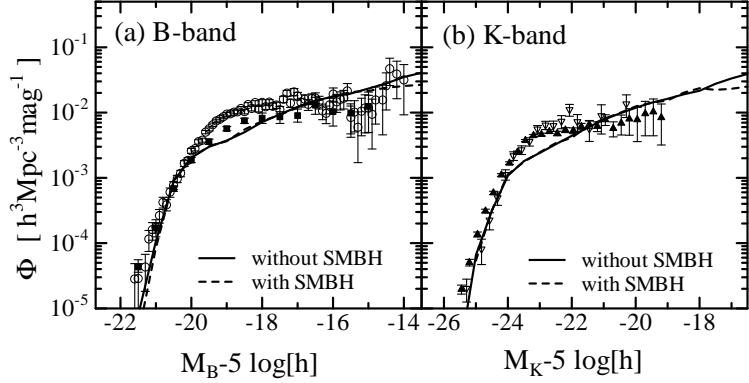


Fig. 1. Local luminosity functions in the (a) B -band and (b) K -band. The thick line shows the result of the model without SMBH formation. The short dashed line shows the model with SMBH formation. Symbols with errorbars in (a) indicate the observational data from APM (Loveday et al. 1992, *filled squares*) and 2dF (Folkes et al. 1999, *open circles*). Symbols in (b) indicate the data from Gardner et al. (1997, *open inverted triangles*), and 2MASS (Cole et al. 2001, *filled triangles*).

populate the bulge of a new galaxy. On the other hand, if $f < f_{\text{bulge}}$, no starburst occurs and a smaller galaxy is simply absorbed into the disk of a larger galaxy. These processes are repeated until the output redshift. We classify galaxies into different morphological types according to the B -band bulge-to-disk luminosity ratio B/D . In this paper, galaxies with $B/D > 2/3$, and $B/D < 2/3$ are classified as ellipticals/S0s and spirals, respectively. This method of type classification well reproduces the observed type mix.

The above procedure is a standard one in the SAM for galaxy formation. Model parameters are determined by comparison with observations of the local Universe. In this study, we use the astrophysical parameters determined by Nagashima et al. (2001) from local observations such as luminosity functions, and galaxy number counts in the Hubble Deep Field. The adopted parameters of this model are tabulated in Table 1. In Figure 1 we plot the results of local luminosity functions of galaxies represented by solid lines. Note that the resultant luminosity functions hardly change if the SMBH formation model is included (dashed lines; see the next section). Symbols with errorbars indicate observational results from the B -band redshift surveys (APM, Loveday et al. 1992; 2dF, Folkes et al. 1999) and from the K -band redshift surveys (Gardner et al. 1997; 2MASS, Cole et al. 2001). As can be seen, the results of our model using these parameters are almost consistent with the observations, at least with the APM result.

3. Model of Quasar Formation

In this section, we introduce a quasar formation and evolution model into our SAM. While this quasar model is similar to that of Kauffmann, Haehnelt (2000), our model of galaxy formation and gas fueling process onto SMBHs is different from theirs.

As mentioned earlier, the masses of SMBHs have tight correlation with the spheroid masses of their host galaxies (e.g. Kormendy, Richstone 1995; Magorrian et al. 1998; Merritt, Ferrarese 2001) and the hosts of quasars found in the local Universe are giant elliptical galaxies or galaxies displacing evidence of major mergers of galaxies (Bahcall et al. 1997). Moreover, in SAMs for galaxy formation, it is assumed that a galaxy-galaxy major merger leads to the formation of a spheroid. Therefore, we assume that SMBHs grow by merging and are fueled by accreted cold gas during major mergers of galaxies. When host galaxies merge, pre-existing SMBHs sink to the center of the new merged galaxy owing to dynamical friction and finally coalesce. The timescale for this process is unknown, but for the sake of simplicity we assume that SMBHs merge instantaneously. Gas-dynamical simulations have demonstrated that the major merger of galaxies can drive substantial gaseous inflows and trigger starburst activity (Negroponte, White 1983; Mihos, Hernquist 1994, 1996; Barnes, Hernquist 1996). Thus, we assume that during major merger, some fraction of the cold gas that is proportional to the total mass of stars newly formed at starburst is accreted onto the newly formed SMBH. Under this assumption, the mass of cold gas accreted on a SMBH is given by

$$M_{\text{acc}} = f_{\text{BH}} \Delta M_{*,\text{burst}}, \quad (5)$$

where f_{BH} is a constant and $\Delta M_{*,\text{burst}}$ is the total mass of stars formed at starburst. $\Delta M_{*,\text{burst}}$ is derived in the Appendix. The free parameter of f_{BH} is fixed by matching the observed relation between a spheroid luminosity and a black hole mass found by Magorrian et al. (1998) and we find that the favorable value of f_{BH} is nearly 0.03. In Figure 2 we show scatterplots (open circles) of the absolute V -band magnitudes of spheroids versus masses of SMBHs of model for $f_{\text{BH}} = 0.03$. The thick solid line is the observational relation and the dashed lines are the 1σ scatter in the observations obtained by Magorrian et al. (1998). The obtained gas fraction ($f_{\text{BH}} = 0.03$) is so small that the inclusion of SMBH formation does not change the properties of galaxies in the local Universe. In Figure 1, the dashed lines show the results of the model with the SMBH formation. This result differs negligibly from the result of the model without SMBH formation. Therefore, we use the same astrophysical parameters tabulated in Table 1 regardless of inclusion of the SMBH formation model. Figure 3 shows black hole mass functions in our model at a series of redshifts. This indicates that the number density of the most massive black holes increases monotonically with time in the scenario where SMBHs grow by accretion of gas and by merging.

Next, we consider the light curve of quasars. We assume that a fixed fraction of the rest mass energy of the accreted gas is radiated in the B -band and the quasar life timescale

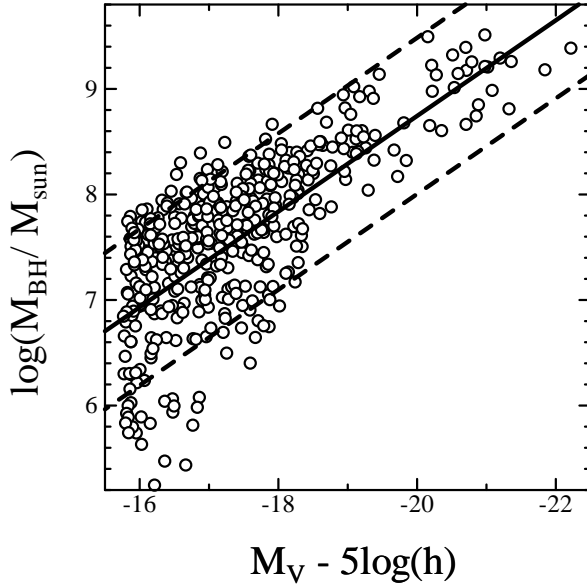


Fig. 2. The relation absolute V -band spheroid magnitude - mass of SMBH. The open circles are an absolute V -band magnitude limited sample of spheroids in our model. The thick solid line is the observational relation obtained by Magorrian et al. (1998). The dashed lines indicate the 1σ scatter in the observations.

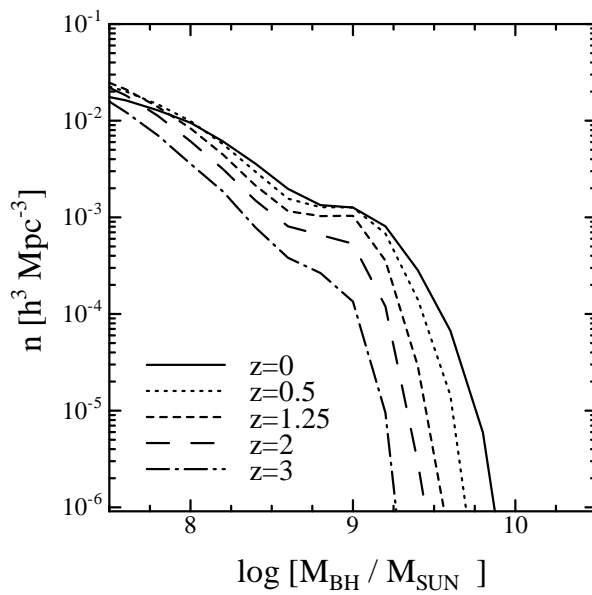


Fig. 3. The black holes mass function of models for $f_{\text{BH}} = 0.03$ as a function of epoch. The solid, dotted, short-dashed, long-dashed and dot-dashed lines indicate the results at $z = 0, 0.5, 1.25, 2$ and 3 respectively.

$t_{\text{life}}(z)$ scales with the dynamical time scale t_{dyn} of the host galaxy. Here we adapt the B -band luminosity of a quasar at time t after the major merger as follows;

$$L_B(t) = L_B(\text{peak}) \exp(-t/t_{\text{life}}). \quad (6)$$

The peak luminosity $L_B(\text{peak})$ is given by

$$L_B(\text{peak}) = \frac{\epsilon_B M_{\text{acc}} c^2}{t_{\text{life}}}, \quad (7)$$

where ϵ_B is the radiative efficiency in B -band, t_{life} is the quasar life timescale and c is the speed of light. In order to determine the parameter ϵ_B and the present quasar life timescale $t_{\text{life}}(0)$, we have chosen them to match our model luminosity function with the observed abundance of bright quasars at $z = 2$. We obtain $\epsilon_B = 0.005$ and $t_{\text{life}}(0) = 3.0 \times 10^7 \text{ yr}$. The resulting luminosity functions at four different redshifts are shown in Figure 4. We superpose the luminosity functions derived from the 2dF 10k catalogue (Croom et al. 2001) for a cosmology with $\Omega_0 = 0.3$, $\lambda_0 = 0.7$ and $h = 0.7$, which is analyzed and kindly provided by T.T. Takeuchi. He used the method of Efstathiou, Ellis, Peterson (1988) for the estimation of the luminosity functions. In order to reanalyze the error with greater accuracy, they applied bootstrap resampling according to the method of Takeuchi, Yoshikawa, Ishii (2000). Absolute B -band magnitudes were derived for the quasars using the k -corrections derived by Cristiani, Vio (1990). Our model reproduces reasonably well the evolution of observed luminosity functions. Thus, in the next section, we use these model parameters in order to investigate the environments of quasars.

For comparison, we also plot the result of model with $\epsilon_B = 0.005$ and $t_{\text{life}}(0) = 3.0 \times 10^8 \text{ yr}$ in Figure 4 (dot-dashed lines). In this case, the abundance of luminous quasars decreases. To prolong a quasar life timescale affects the quasar luminosity function due to the following two factors: a decrease in the peak luminosity L_B (eq.[7]) and an increase in the exponential factor $\exp(-t/t_{\text{life}})$ in equation (6). For the majority of bright quasars, the elapsed time t since the major merger is much smaller than the quasar life timescale t_{life} , $t/t_{\text{life}} \ll 1$. Therefore, the former factor dominates the latter and the number of luminous quasars decreases. Thus, a long quasar life timescale results in a very steep quasar luminosity function. Note that if we change the radiative efficiency ϵ_B , the quasar luminosities simply scale by a constant factor in our model. Thus, changing ϵ_B shifts the luminosity function horizontally.

4. Environments of Quasars

In this section, we investigate the environments of quasars using our model. We consider the halo mass dependence of the mean number of quasars per halo and the probability distribution of the number of galaxies around quasars as characterizations of the environments of quasars. This is because the former is one of measures of the relation between quasars and dark matter distributions and the latter reflects the relationship between galaxies and quasars.

In Figure 5, we plot $\langle N_{\text{gal}}(M) \rangle$ and $\langle N_{\text{QSO}}(M) \rangle$ that denote the mean number of galaxies

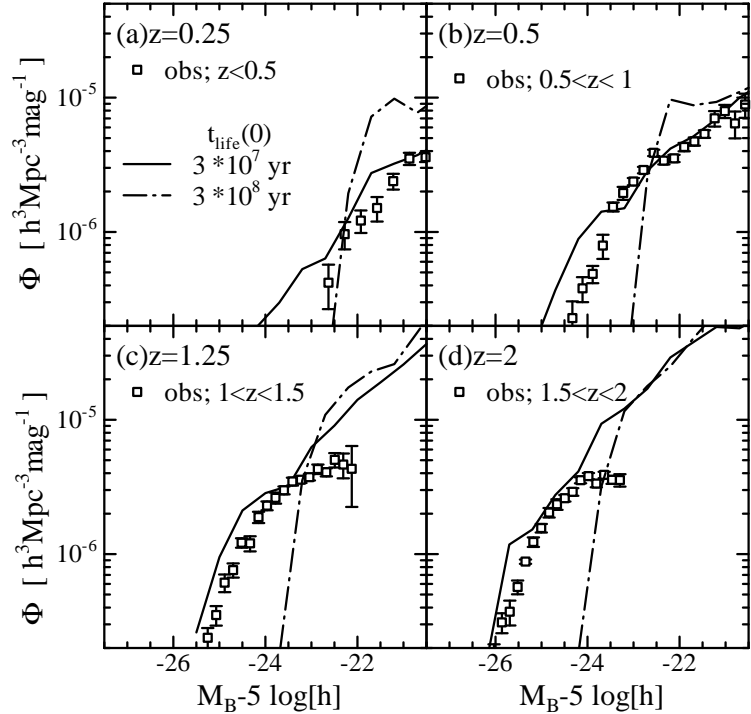


Fig. 4. The B -band quasar luminosity functions at (a) $z = 0.25$, (b) $z = 0.5$, (c) $z = 1.25$ and (d) $z = 2.0$. The solid lines are $t_{\text{life}}(0) = 3 \times 10^7 \text{ yr}$ and the dot-dashed lines are $t_{\text{life}}(0) = 3 \times 10^8 \text{ yr}$. The symbols show results from the 2dF 10k catalogue (Croom et al. 2001) reanalyzed by Takeuchi for a cosmology $\Omega_0 = 0.3, \lambda_0 = 0.7$ and $h = 0.7$.

and quasars per halo with mass M , respectively, at (a) $z = 0.5$ and (b) $z = 2.0$. We select galaxies with $M_B - 5 \log(h) < -19$ and quasars with $M_B - 5 \log(h) < -21$. It should be noted that changing the magnitude of selection criteria for galaxies and quasars would alter these results, but qualitative features are not altered. As is seen in Figure 5, there are more galaxies and quasars at high z . At higher redshift, halos have more cold gas available to form stars and to fuel SMBHs. Thus, the number of luminous galaxies grows. Furthermore, at higher redshift, both timescales of the dynamical friction and the random collisions are shorter because the mass density of a halo is higher. Therefore, the galaxy merging rate increases. Consequently, the number of quasars also grows. Moreover, the decrease in the quasar life timescale t_{life} with redshift also contributes to the increase in the number of quasars because quasars become brighter as a result of decrease in t_{life} (eq. [7]).

From Figure 5, we find that the dependence of $\langle N_{\text{QSO}}(M) \rangle$ on halo mass M is different from the dependence of $\langle N_{\text{gal}}(M) \rangle$. Furthermore, Figure 6 shows that the ratio of $\langle N_{\text{QSO}}(M) \rangle$ to $\langle N_{\text{gal}}(M) \rangle$ varies with redshift and halo mass. Some studies of galaxy clustering show that the bias in the galaxy spatial distribution relative to the mass spatial distribution is highly sensitive to the numbers of galaxies in halos of different mass (Benson et al. 2000, Seljak 2000). This result is applicable to the bias in the quasar spatial distribution. Therefore, these results

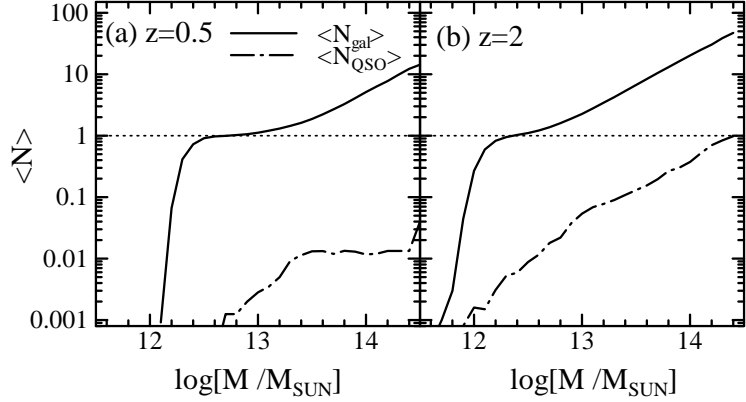


Fig. 5. The mean numbers of galaxies with $M_B - 5 \log(h) < -19$ (solid lines) and quasars with $M_B - 5 \log(h) < -21$ (dot-dashed lines) per halo with mass M at (a) $z = 0.5$ and (b) $z = 2.0$. The horizontal dotted line marks $\langle N_{\text{gal}} \rangle = 1$ and $\langle N_{\text{QSO}} \rangle = 1$

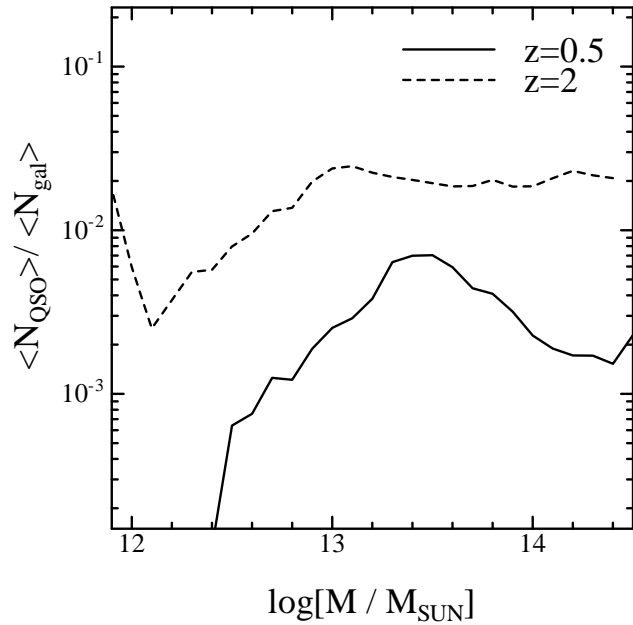


Fig. 6. The ratio of the mean number of galaxies with $M_B - 5 \log(h) < -19$ to the mean number of quasars with $M_B - 5 \log(h) < -21$ per halo with mass M at $z = 0.5$ (solid line) and $z = 2.0$ (dot-dashed line).

of our model suggest that the clustering of galaxies is not the same as the clustering of quasars.

Next, we formulate the conditional probability that a halo with N_{QSO} quasars has N_{gal} galaxies. The number density of the halos which contains N_{gal} galaxies and N_{QSO} quasars at z is obtained from the following expression:

$$n(N_{\text{gal}}, N_{\text{QSO}}|z) = \int N(N_{\text{gal}}, N_{\text{QSO}}|M, z) n(M|z) dM \quad (8)$$

where $N(N_{\text{gal}}, N_{\text{QSO}}|M, z) dN_{\text{gal}} dN_{\text{QSO}}$ denotes the number of the halos with mass M which

contains $N_{\text{gal}} \sim N_{\text{gal}} + dN_{\text{gal}}$ galaxies and $N_{\text{QSO}} \sim N_{\text{QSO}} + dN_{\text{QSO}}$ quasars at z and $n(M|z)$ is the dark halos mass function at z . Our SAM adopts the Press-Schechter mass function which is given by

$$n(M|z)dM = \sqrt{\frac{2}{\pi}} \frac{\rho_0}{M} \frac{\delta_c(z)}{\sigma^2(M)} \left| \frac{d\sigma(M)}{dM} \right| \exp \left[-\frac{1}{2} \frac{\delta_c^2(z)}{\sigma^2(M)} \right] dM, \quad (9)$$

where ρ_0 is the present mean density of the universe, $\sigma(M)$ is the rms liner density fluctuation on the scale M at $z=0$ and $\delta_c(z)$ is the critical density contrast for collapse at z , extrapolated to the present time using liner theory. The number density of the halos which contain N_{QSO} quasars at z is obtained from the following expression:

$$n(N_{\text{QSO}}|z) = \int N(N_{\text{QSO}}|M, z) n(M|z) dM \quad (10)$$

where $N(N_{\text{QSO}}|M, z)dN_{\text{QSO}}$ denotes the number of the halos with mass M which contain $N_{\text{QSO}} \sim N_{\text{QSO}} + dN_{\text{QSO}}$ quasars at z . From equation (8) and (10), the conditional probability that the halo with N_{QSO} quasars has $N_{\text{gal}} \sim N_{\text{gal}} + dN_{\text{gal}}$ galaxies at z is given by

$$P(N_{\text{gal}}|N_{\text{QSO}}, z)dN_{\text{gal}} = \frac{n(N_{\text{gal}}, N_{\text{QSO}}|z)}{n(N_{\text{QSO}}|z)} dN_{\text{gal}}. \quad (11)$$

As is seen in the above formulation, given $N(N_{\text{gal}}, N_{\text{QSO}}|M, z)$ and $N(N_{\text{QSO}}|M, z)$ from the quasar formation model, one can calculate the probability distribution for the numbers of galaxies around quasars.

Figure 7 shows these galaxy number distribution functions around quasars estimated by our model. The results are shown for quasars brighter than $M_B - 5\log(h) = -22$ and for galaxies brighter than $M_B - 5\log(h) = -19$. Note that at $z = 0.25$ and $z = 0.5$ $P(N_{\text{gal}}|N_{\text{QSO}} = 2) = 0$ and $P(N_{\text{gal}}|N_{\text{QSO}} = 3) = 0$ for all N_{gal} (Fig. 7(a) and (b)) and that at $z = 1.25$ $P(N_{\text{gal}}|N_{\text{QSO}} = 3) = 0$ for all N_{gal} (Fig. 7(c)). At a lower redshift, a halo has at most one quasar. Fig 7(a) and (b) show that the halo which has one quasar contains several galaxies by high probability. These results indicate that most quasars tend to reside in groups of galaxies at $0.2 \lesssim z \lesssim 0.5$ and is consistent with the observation at $z \lesssim 0.4$ (e.g. Bahcall, Chokshi 1991; Fisher et al. 1996; McLure, Dunlop 2001). On the other hand, at a higher redshift, the numbers of galaxies in the halo with one or two quasars is from several to dozens (Fig 7(c) and (d)). These results indicate that quasars locate in ranging from small groups of galaxies to clusters of galaxies. Thus at $1 \lesssim z \lesssim 2$ quasars seem to reside in more varied environments than at a lower redshift.

5. Summary and Discussion

We have constructed a unified semi-analytic model for galaxy and quasar formation and have predicted the mean number of quasars per halo with mass M , $\langle N_{\text{QSO}}(M) \rangle$, and probability distribution of the number of galaxies around quasars, $P(N_{\text{gal}}|N_{\text{QSO}})$, as characterizations of the environments of quasars. These quantities reflect the processes of quasar formation such as the amount of cold gas available for fueling, the galaxy merger rate and the quasar life

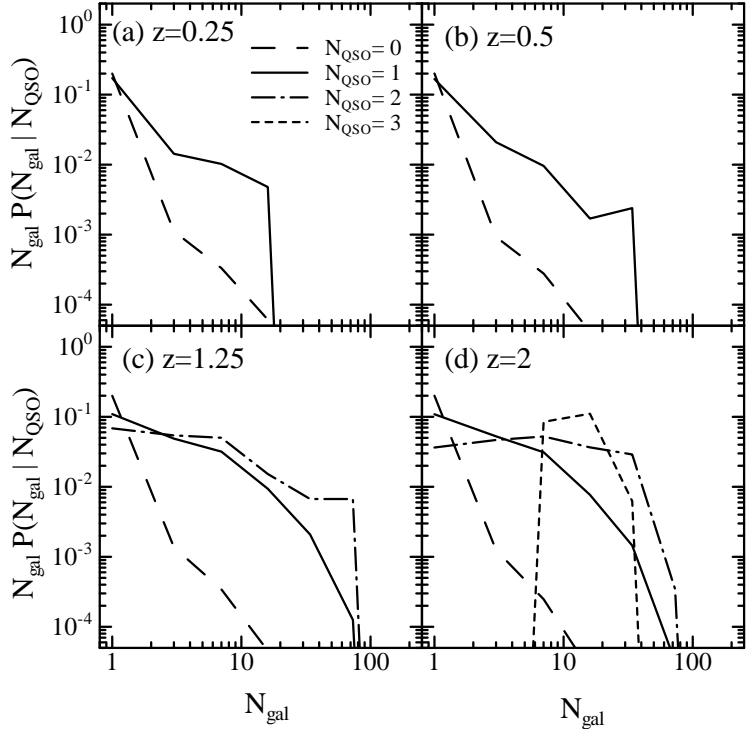


Fig. 7. The probability distribution for the numbers of galaxies around quasars (a) $z = 0.25$, (b) $z = 0.5$, (c) $z = 1.25$ and (d) $z = 2.0$. The selected galaxies are brighter than $M_B - 5 \log(h) = -19$ and the selected quasars are brighter than $M_B - 5 \log(h) = -22$. Long-dashed, solid, dot-dashed and short-dashed lines show results for $N_{\text{QSO}} = 0.25, 0.5, 1.25$ and 2 respectively.

timescale. Therefore, by comparing these predictions with observations, one will be able to constrain quasar formation models.

In our model, we have assumed that the merger remnant becomes a spheroid when two galaxies of comparable masses merge (major merger). During the major merger, a starburst takes place and some fraction of cold gas in the merger remnant is accreted onto an SMBH over a timescale that scales as the dynamical time of the host galaxy. We have assumed that the accreted gas fraction is proportional to the total mass of stars formed at starburst. Our model can reproduce the observed relation of the SMBH mass to spheroid luminosity and the quasar luminosity functions at different redshifts (Fig.2 and Fig.4). The accreting gas fraction ($f_{\text{BH}} = 0.03$) is so small that SMBH formation does not affect properties of galaxies in the local Universe such as the luminosity functions of galaxies (Fig.1). Thus, we adopt the same astrophysical parameters of galaxy formation as those without SMBH formation. Using this model, we have shown $\langle N_{\text{QSO}}(M) \rangle$ and $P(N_{\text{gal}} | N_{\text{QSO}})$.

The ratio of $\langle N_{\text{QSO}}(M) \rangle$ to $\langle N_{\text{gal}}(M) \rangle$ varies with halo mass in our model (Fig5). Benson et al. (2000) used a combination of cosmological N -body simulation and semi-analytic modeling of galaxy formation and showed that the galaxy spatial distribution is sensitive to the efficiency with which galaxies form in halos with different mass. Seljak (2000) also obtained the same

conclusion using an analytic model of galaxy clustering. These results are applicable to the quasar spatial distribution. Therefore, our result indicates that the clustering properties of galaxies is not the same as those of quasars and that the bias in the spatial distribution of galaxies relative to that of dark matter is not the same as the bias in the spatial distribution of quasars.

At lower redshifts ($0.2 \lesssim z \lesssim 0.5$), our prediction of galaxy number distribution function around quasars, $P(N_{\text{gal}}|N_{\text{QSO}})$, shows most halos which have quasars have at most several galaxies (Fig.7(a) and (b)). This indicates that most quasars reside in groups of galaxies and agrees with the observation at $z \lesssim 0.4$. On the other hand, at higher redshift, ($1 \lesssim z \lesssim 2$), the number of galaxies in the halo with quasars is from several to dozens (Fig.7(c) and (d)); quasars reside in ranging from small groups of galaxies to clusters of galaxies. This indicates that most quasars at higher redshift reside in more varied environments than at lower redshift. This model prediction is checkable by statistics of galaxies around quasars which will be obtained in future.

It is still controversial whether the environments of quasars depend on their optical and radio luminosities. Some authors have claimed that radio-loud quasars were located in richer environments than radio-quiet quasars at $z < 0.6$ (e.g. Yee, Green 1984; Yee, Green 1987; Ellingson, Yee, Green 1991; Hintzen, Romanishin, Vlades 1991). However, other people obtained a different result. For example, Hutchings, Crampton, Johnson (1995) observed the galaxy environment of radio-loud quasars and radio-quiet quasars and concluded that there is no significant difference in the richness. Recent studies support this conclusion (e.g. Wold et al. 2001). The discrepancies between different studies may be caused partly by too small quasar samples and by differences in sample selection of quasars. This situation will soon improve with the availability of a new generation of very large quasar surveys such as the 2dF quasar redshift survey (Croom et al. 2001) and the Sloan Digital Sky Survey (York et al. 2000). Although we do not deal with radio properties of quasars in this paper, our investigation of quasar environments will also provide a clue for understanding the radio character of quasar environments.

The mean number of quasars per halo, $\langle N_{\text{QSO}}(M) \rangle$, and probability distribution of the number of galaxies around quasars, $P(N_{\text{gal}}|N_{\text{QSO}})$, used in this study can provide some useful features of the quasar environments. Furthermore, the spatial galaxy-quasar correlation function is used in order to quantify the galaxy environments around a quasar. Therefore, for the further investigation of environments and clustering of quasars and in order to constrain the quasar formation model, it is also necessary to predict spatial distribution of galaxies and quasars (Kauffmann, Haehnelt 2002). We will show the results using the combination of cosmological N -body simulation and SAM for formation of galaxy and quasar in the near future.

We would like to thank T.T. Takeuchi for providing us with the reanalyzed data of the quasar luminosity functions derived from the 2dF 10k catalogue. We are also grateful

to K. Okoshi, H. Yahagi and S. Yoshioka for useful comments and discussions. Numerical computations in this work were partly carried out at the Astronomical Data Analysis Center of the National Astronomical Observatory, Japan. This work has been supported in part by the Grant-in-Aid for the Scientific Research Funds(13640249) of the Ministry of Education, Culture, Sports, Science and Technology of Japan.

Appendix. Star Formation and Gas Evolution

In this appendix, we summarize our model of star formation and gas evolution. We use a simple instantaneous recycling approximation of model star formation, feedback and chemical enrichment. The following difference equations describe the evolution of the mass of cold gas M_{cold} , hot gas M_{hot} , and long lived stars M_{star} at each time step.

$$\dot{M}_{\text{cold}} = -\dot{M}_* + R\dot{M}_* - \beta\dot{M}_*, \quad (\text{A1})$$

$$\dot{M}_{\text{hot}} = \beta\dot{M}_*, \quad (\text{A2})$$

$$\dot{M}_{\text{star}} = \dot{M}_* - R\dot{M}_*, \quad (\text{A3})$$

where $\dot{M}_* = M_{\text{cold}}/\tau_*$ is star formation rate, R is the gas fraction returned by evolved stars, and β is the efficiency of reheating. In this paper, $R = 0.25$. The solutions of these equations are the following:

$$M_{\text{cold}} = M_{\text{cold}}^0 \exp \left[- (1 - R + \beta) \frac{t}{\tau_*} \right], \quad (\text{A4})$$

$$M_{\text{hot}} = M_{\text{hot}}^0 + \beta \Delta M_*, \quad (\text{A5})$$

$$M_{\text{star}} = M_{\text{star}}^0 + (1 - R) \Delta M_*, \quad (\text{A6})$$

where M_{cold}^0 , M_{hot}^0 , M_{star}^0 and M_{BH}^0 are the masses of cold gas, hot gas, long-lived stars and black holes mass from the previous time step, t is the time sine the start of the time step, and $\Delta M_* = (M_{\text{cold}}^0 - M_{\text{cold}})/(1 - R + \beta)$ is the mass of total formed stars.

When a starburst occurs, stars are formed in a very short timescale. Thus, the starburst corresponds to $\tau_*/t \rightarrow 0$ in the above solutions. In this case, the changes of masses are given by

$$M_{\text{cold}} = 0, \quad (\text{A7})$$

$$M_{\text{hot}} = M_{\text{hot}}^0 + \frac{(1 - R) M_{\text{cold}}^0}{1 - R + \beta}, \quad (\text{A8})$$

$$M_{\text{star}} = M_{\text{star}}^0 + \frac{\beta M_{\text{cold}}^0}{1 - R + \beta} \quad (\text{A9})$$

and the total star mass formed at starburst becomes

$$\Delta M_{*,\text{burst}} = \frac{M_{\text{cold}}^0}{1 - R + \beta}. \quad (\text{A10})$$

From equation (A10), we can obtain the mass of accreted cold gas onto a black hole (eq.[5]).

References

Bahcall, J. N., Schmidt, M., & Gunn, J. E. 1969, *ApJL*, 157, L77

Bahcall, N. A., & Chokshi, A. 1991, *ApJL*, 380, L9

Bahcall, J. N., Kirhakos, S., Saxe, D. H., & Schneider, D. P. 1997, *ApJ*, 479, 642

Bardeen, J. M., Bond, J. R., Kaiser, N., & Szalay, A. S. 1986, *ApJ*, 304, 15

Barnes, J. E. 1988, *ApJ*, 331, 699

Barnes, J. E., & Hernquist, L. 1996, *ApJ*, 471, 115

Benson, A. J., Cole, S., Frenk, C. S., Baugh C. M., & Lacey, C. G. 2000, *MNRAS*, 311, 793

Binney, J., & Tremaine, S. 1987, *Galactic Dynamics*, Princeton Univ. Press, Princeton, NJ

Bond, J. R., Cole, S. , Efstathiou, G., & Kaiser, N. 1991, *ApJ*, 379, 440

Bower, R. J. 1991, *MNRAS*, 248, 332

Cattaneo, A. 2001, *MNRAS*, 324, 128

Cole, S., Aragon-Salamanca, A., Frenk, C. S., Navarro, J. F., & Zepf, S. E. 1994, *MNRAS*, 271, 781

Cole, S., Lacey, C. G., Baugh, C. M., & Frenk, C. S. 2000, *MNRAS*, 319, 168

Cole, S., Norberg, P., Baugh, C. M., Frenk, C. S., Bland-Hawthorn, J., Bridges, T., Cannon, R., Colless, M., et al. 2001, *MNRAS*, 326, 255

Cristiani, S. & Vio, R. 1990, *A&A*, 227, 385

Croom, S. M., Smith, R. J., Boyle, B. J., Shanks, T., Loaring, N. S., Miller, L., & Lewis, I. J., 2001, *MNRAS*, 322, L29

Efstathiou, G., Ellis, R. S., & Peterson, B. A. 1988, *MNRAS*, 232, 431

Efstathiou, G. & Rees, M. J., 1988, *MNRAS*, 230, P5

Ellingson, E., Yee H. K. C., & Green, R. F., 1991, *ApJ*, 371, 49

Fisher, K. B., Bahcall, J. N., Kirhakos, S., & Schneider, D. P., 1996, *ApJ*, 468, 469

Folkes, S., Ronen, S., Price, I., Lahav, O., Colless, M., Maddox, S., Deeley, K., Glazebrook, K., et al. 1999, *MNRAS*, 308, 459

Gardner, J. P., Sharples, R. M., Frenk, C. S., & Carrasco, B. E. 1997, *ApJL*, 480, L99

Haehnelt, M., & Rees, M. J., 1993, *MNRAS*, 263, 168

Haehnelt, M., Natarajan, P. & Rees, M. J., 1998, *MNRAS*, 300, 817

Haiman, Z., & Loeb, A., 1998, *ApJ*, 503, 505

Hernquist, L. 1992, *ApJ*, 400, 460

Hernquist, L. 1993, *ApJ*, 409, 548

Heyl, J.S., Hernquist, L., & Spergel, D. 1994, *ApJ*, 427, 165

Hintzen, P., Romanishin, W., & Valdes, F., 1991, *ApJ*, 366, 7

Hosokawa, T., Mineshige, S., Kawaguchi, T., Yoshikawa, K., & Umemura, M. 2001, *PASJ*, 53, 861

Hutchings, J. B., Crampton, D., & Johnson, A., 1995, *AJ*, 109, 73

Kauffmann, G., White, S.D.M. & Guiderdoni, 1993, *MNRAS*, 264, 201

Kauffmann, G., & Charlot, S., 1998, *MNRAS*, 297, 23

Kauffmann, G., & Haehnelt, M. 2000, *MNRAS*, 311, 576

Kauffmann, G., & Haehnelt, M. 2002, *MNRAS*, 332, 529

Kodama, T., & Arimoto, N. 1997, *A&A*, 320, 41

Kormendy, J., & Richstone, D., 1995, *ARA&A*, 33, 581

Lacey, C. G., & Cole, S. 1993, MNRAS, 262, 627

Loveday, J., Peterson, B. A., Efstathiou, G., & Maddox, S. J. 1992, ApJ, 90, 338

Lynden-Bell, D. 1969, Nature, 223, 690

Magorrian, J., Tremaine, S., Richstone, D., Bender, R., Bower, G., Dressler, A., Faber, S. M., Gebhardt, K., et al., 1998, AJ, 115, 2285

Makino, J., & Hut, P. 1997, ApJ, 481, 83

McLure, R. J., & Dunlop, J. S. 2001, MNRAS, 321, 515

Merritt, D., & Ferrarese, L. 2001, MNRAS, 320, L30

Mihos, J., & Hernquist, L., 1994, ApJL, 431, L9

Mihos, J., & Hernquist, L., 1996, ApJ, 464, 641

Nagashima, M., & Gouda, N. 2001, MNRAS, 325, L13

Nagashima, M., Totani, T., Gouda, N., & Yoshii, Y. 2001, ApJ, 557, 505

Nagashima, M., Yoshii, Y., Totani, T., & Gouda, N. 2002, ApJ, in press

Negroponte, J., & White, S. D. M., 1983, MNRAS, 205, 1009

Press, W. H., & Schechter, P. 1974, ApJ, 187, 425

Seljak, U. 2000, MNRAS, 318, 203

Shimizu, M., Kitayama, T., Sasaki, S., & Suto, Y. 2002, PASJ, in press (astro-ph/0207230)

Somerville, R. S., & Kolatt, T. 1999, MNRAS, 305, 1

Somerville, R. S., & Primack, J. R. 1999, MNRAS, 310, 1087

Takeuchi, T. T., Yoshikawa, K., & Ishii, T. T. 2001, ApJS, 129, 1

Wold, M., Lacy, M., Lilje, P.B., & Serjeant, S. 2001, MNRAS, 323, 231

Yee H.K.C., & Green, R.F., 1984, ApJ, 280, 79

Yee H.K.C., & Green, R.F., 1987, ApJ, 319, 28

York, D. G., Adelman, J., Anderson, J. E. Jr., Anderson, S. F., Annis, J., Bahcall, N. A., Bakken, J. A., Barkhouser, R., et al., 2000, AJ, 120, 1579